

Percolative effects in oxygen-depleted $\text{YBa}_2\text{Cu}_3\text{O}_x$ wires

B. S. Palmer* and H. D. Drew

Laboratory for Physical Sciences, College Park, Maryland, 20740, USA

R. A. Hughes and J. S. Preston

Department of Engineering Physics, McMaster University, Hamilton, Ontario, Canada, L8S 4L8

(Received 9 August 2004; published 15 November 2004)

The superconducting transition is studied in wires “written” in oxygen-depleted $\text{YBa}_2\text{Cu}_3\text{O}_x$ ($x \sim 6.4$) thin films by photodoping with a near-field scanning optical microscope. The enhancement of the superconducting transition temperature observed for wide wires is found to be suppressed for wires below a sample dependent width ($\sim 1-2 \mu\text{m}$). This behavior is understood in terms of percolation of the supercurrent through an inhomogeneous distribution of weak links in these samples grown by pulsed laser deposition. As the wire width is reduced the highest T_c percolation path is cut off, leading to a lower T_c . By modeling the electronic transport data and T_c versus wire width data using a classical bond percolation model and the Ambegaokar-Halperin thermally activated phase-slip theory for a weak link, we conclude that the density of weak links in these samples is approximately 1 weak link/ μm .

DOI: 10.1103/PhysRevB.70.184511

PACS number(s): 74.78.Bz, 74.50.+r, 68.37.Uv

I. INTRODUCTION

In part, the great interest in the underdoped high- T_c superconductors is because of the exotic behaviors exhibited via many of the physical properties that have been observed in these materials in this range of the phase diagram (e.g., the pseudogap, the loss of phase coherence, and the Nernst effect).¹⁻³ The attempt to understand these results has led to many theoretical speculations. These different theories include a quantum critical point at the superconducting-“insulator” transition, spin and charge inhomogeneities (“stripes”), and fluctuations in the phase of the order parameter that controls the observed T_c in the underdoped region. Some of these predictions concern fundamentally new states in condensed matter physics; that is, they have not been observed in conventional metal physics. However, the effect of disorder in this region of the phase diagram must also be considered.

A particularly interesting method for investigating the underdoped phase of the high- T_c superconductors is by varying the T_c continuously, in the same sample, with light via the photoconductivity effect. The oxygen-deficient (underdoped) $\text{RBa}_2\text{Cu}_3\text{O}_x$ superconductors (with R being a rare-earth element) exhibit persistent photoconductivity; for $\text{YBa}_2\text{Cu}_3\text{O}_x$ (YBCO) the changes induced with light persist over approximately 24 h at room temperature and are essentially permanent below 250 K.⁴ While the exact physical mechanism of photoconductivity in underdoped YBCO is still not fully understood,⁵ the effect is found to be analogous to increasing the oxygen concentration of the material and is thus called “photodoping.” The resistivity decreases, the superconducting transition temperature T_c increases (measured by resistance and magnetization techniques),⁴ the reflectivity of the sample changes, and the c axis has also been observed to contract after illumination.^{6,7}

In the work described in this article, we used a near-field scanning optical microscope (NSOM) to photodope oxygen-depleted YBCO thin films and studied the superconducting

properties of wires “written” in the samples. This work was initially motivated by the work of Decca *et al.*, in which photoinduced superconducting nanowires and Josephson junctions were created in GBCO and YBCO.⁸ We find that the large enhancement of the superconducting transition temperature observed for wide wires is not found for wires narrower than a sample dependent width $1-2 \mu\text{m}$. From our observations of the behavior of T_c versus wire width, we conclude that the superconducting properties of these films are dominated by percolation. Since the percolative path is cut off when a narrow photoinduced wire is made with the NSOM, the observed macroscopic T_c is not enhanced. The inhomogeneities are believed to be weak links associated with grain boundaries in the material. Modeling the transport data using a classical bond percolation model and an Ambegaokar-Halperin thermal activation theory for a weak link, we conclude that the density of inhomogeneities or weak links is approximately 1 weak link/ μm .

Details of the samples and experiment are discussed in the following section. Section III presents the experimental results on the samples. An analysis of the results is presented in Sec. IV.

II. SAMPLES AND EXPERIMENT

The YBCO thin films (thickness $\approx 100 \text{ nm}$) studied here were grown optimally doped ($x=7-\delta$) by pulsed-laser deposition on SrTiO_3 . The samples were patterned and etched for four-point resistance or I - V measurements using standard photolithographic techniques. The current channel was $10 \mu\text{m}$ wide and the voltage leads had an inner separation of $4 \mu\text{m}$ with an outer separation of $10 \mu\text{m}$. After completing the lithography, the resistance versus temperature from 77 to 300 K was measured. The resistivity was linear near 300 K with a slope that varied from $0.94-1.2 \mu\Omega \text{ cm/K}$ and the T_c 's were greater than 90 K with widths less than 0.5 K . These properties attest to high quality of films after processing.⁹

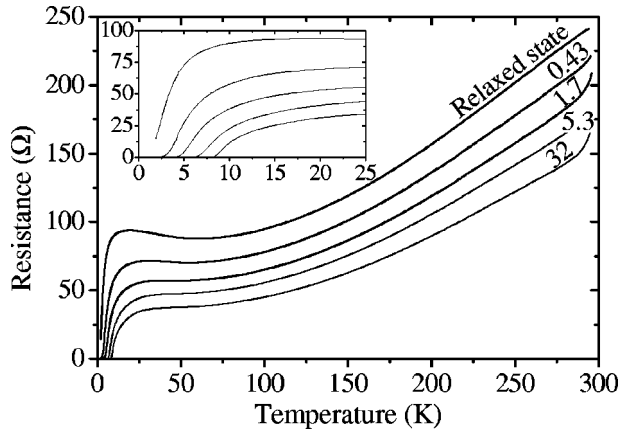


FIG. 1. Resistance versus temperature for a typical sample in its relaxed state and after photodoping the entire sample using a different integrated number of photons specified by the numbers (W min/cm^2) associated with each curve. Inset of figure shows a blowup at lower temperatures.

The samples were then oxygen annealed to an oxygen stoichiometry near $x=6.4$. To perform the oxygen anneal, the oxygen partial pressure was controlled from 10 Torr to 20 mTorr as a function of temperature to follow a P_{O_2} - T curve that maintains a constant oxygen stoichiometry in the sample.^{10,11}

Following the oxygen anneal, the samples were first characterized in the far field to measure the photon dose ($\lambda = 632.8 \text{ nm}$) required to induce changes in the sample, the changes in resistance of the sample, and the total change in the superconducting transition temperature. It was found that after a photon dose of 2×10^{21} photons/ cm^2 (corresponding to illuminating the sample for 10 min using an irradiance of 1 W/cm^2), the changes in the sample had nearly saturated.⁴ The state of the sample for photon doses greater than 2×10^{21} photons/ cm^2 , is defined in this paper as a “quasisaturated photodoped state.” While the state of the sample before the illumination began or after a room temperature anneal of several days is defined as the “relaxed state.” When photodoping with the NSOM, Al-coated tapered optical fiber tips with apertures approximately 125 nm in diameter were used.¹² To expedite the photodoping process with the NSOM, an irradiance of 200–1000 W/cm^2 was used in the near-field.

Since the photocarriers are long lived at room temperature, all of the photodoping described in this paper was done at room temperature. To perform resistance versus temperature measurements, the sample was placed in a Dewar and cooled to below 250 K (at which temperature changes induced in the sample are permanent) within 15 min after the illumination had ceased. Figure 1 shows a typical set of resistance versus temperature curves after photodoping the whole sample with different photon doses as specified by the numbers (W min/cm^2) associated with each curve.

III. RESULTS

We report results on two samples. However similar results were observed in other samples with a variety of dopings

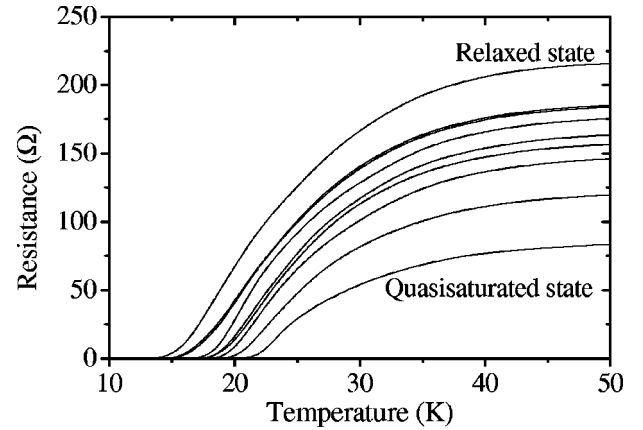


FIG. 2. Resistance versus temperature for different photodoped wire widths for sample A. The different wire widths in order of decreasing resistance, at constant temperature, are relaxed state, 0.5, 0.75, 1, 1.5, 2, 2.75, 4 μm , and quasisaturated state.

($1.5 \text{ K} < T_c < 20 \text{ K}$). Sample A had a $T_c = 13 \text{ K}$ in its relaxed state and a $T_c = 20.5 \text{ K}$ for wide wires in its quasisaturated state.¹³ Figure 2 shows the resistance versus temperature for photodoped wires, with different widths, which were photodoped to the quasisaturated state. To make wider wires, a wire is first “written” with the NSOM parallel to the current channel and then moved perpendicular to the current channel. The sizes of the wires are estimated from the writing process and from the changes in the resistance. Figure 3 is a plot of T_c for sample A as a function of wire width. As this figure shows, a large enhancement of T_c was not observed for wire widths smaller than $1 \mu\text{m}$.

The second sample we will discuss, sample B, had a $T_c = 1.5 \text{ K}$ in its relaxed state, and after photodoping wide wires to their quasisaturated state, had a $T_c = 15.2 \text{ K}$. Figure 4 shows T_c versus wire width for sample B for two levels of integrated irradiance. The data denoted as squares had the sample photodoped to its quasisaturated state. For the data denoted as circles, the sample was photodoped with 1/6 the integrated irradiance of the quasisaturated state. For wires

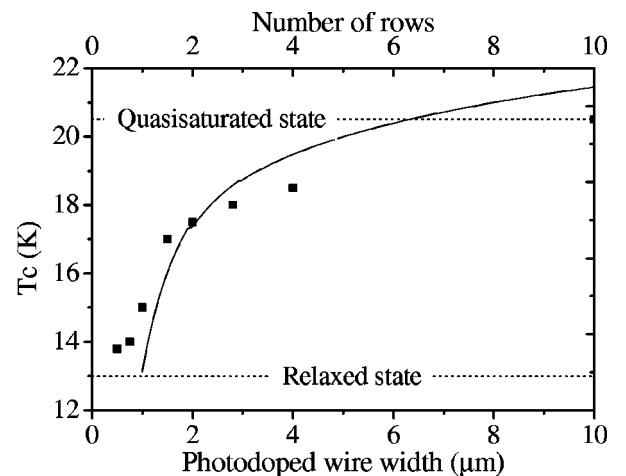


FIG. 3. T_c versus photodoped wire width for sample A. Data are from Fig. 2. The line is a model calculation based on a classical bond percolation model.

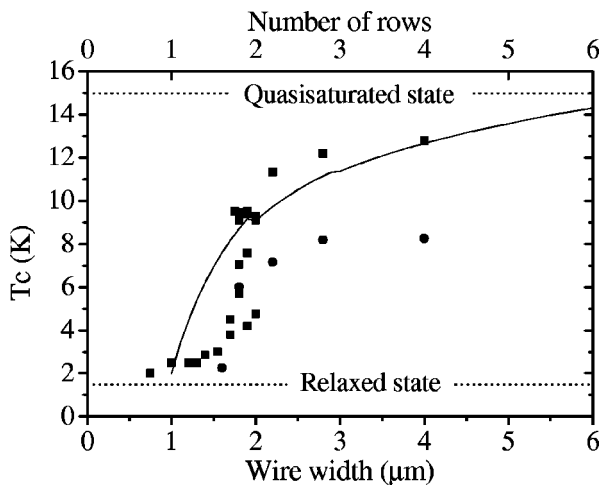


FIG. 4. T_c versus photodoped wire width for sample B for two different integrated photon densities. The sample was photodoped to its quasisaturated state for the data denoted as squares. For the data denoted as circles, the sample was photodoped with $1/6$ the integrated irradiance used to photodope it to its quasisaturated state. The line is a model of the data based on a classical bond percolation model.

narrower than $1.8 \mu\text{m}$, no large enhancement in the superconducting transition temperature was observed for this sample.

IV. ANALYSIS

The data on the underdoped YBCO thin-film samples presented in the last section showed a suppression in the superconducting transition temperature of the photogenerated wires when their width was reduced below $\sim 1\text{--}2 \mu\text{m}$. Several mechanisms that could suppress the enhancement of the superconducting temperature in narrow wires were considered. These include the proximity effect, fluctuation effects, and percolative effects due to inhomogeneities in the films.

Since the length scale for the suppression of T_c in these wires is approximately $1 \mu\text{m}$, which is much larger than the coherence length ($\xi \approx 1 \text{ nm}$), a conventional proximity effect or a thermally activated phase slip theory for narrow superconducting wires cannot explain these results.

A. Phase fluctuations

Another model that was considered in attempting to explain the suppression of T_c in the narrow photoinduced wires was based on Emery and Kivelson's phase fluctuation model of the cuprates.¹ In this model, the superconducting transition temperature for the underdoped cuprates is proportional to the zero temperature phase stiffness $V_o \propto 1/\lambda^2(0)$. This model is consistent with the observation by Uemura *et al.* that the superconducting transition temperature for the underdoped cuprates is proportional to the inverse of the superconducting penetration depth squared ($T_c \propto \lambda^{-2}$).¹⁴

Based on this model, we hypothesized that underdoped YBCO wires with a width smaller than the London penetration depth may have a reduced phase stiffness and hence a

smaller T_c than a wire wider than the London penetration depth. The London penetration depth for bulk YBCO with a $T_c = 10 \text{ K}$ is estimated, using the Uemura result,¹⁴ to be $\lambda_{ab}(T_c = 10 \text{ K}) = (\sqrt{56}/10)\lambda_{ab}(T_c = 56 \text{ K}) = 480 \text{ nm}$, where $\lambda_{ab}(T_c = 56 \text{ K}) = 200 \text{ nm}$ was measured by an absolute muon spin relaxation technique.¹⁵ An estimate of the effective superconducting penetration depth for a $t = 100\text{-nm}$ -thick film with a T_c of 10 K is $\lambda_{\perp} = \lambda^2/t \approx 2.25 \mu\text{m}$, which is very close to the observed critical wire width in Figs. 3 and 4.

This hypothesis was tested by using the capability to tune the superconducting transition temperature of these samples. By illuminating the underdoped YBCO samples with a different integrated number of photons and tuning the superconducting transition temperature, the Uemura result implies that the London penetration depth also effectively changes with T_c .

If the critical width to suppress the superconducting transition temperature of the photoinduced wires is controlled by the London penetration depth, then that critical width should change if we "write" wires using a different integrated number of photons. In particular, a wire photodoped with a smaller integrated number of photons will have a smaller T_c , and a longer penetration depth, so that the critical width to suppress T_c should be greater.

To perform this test, wires were photodoped in sample B with $\approx 1/6$ the integrated irradiance used to photodope the quasisaturated wires in Fig. 4. The data for this test are shown in Fig. 4 and show no measurable increase in the critical width. Based on the ratio of the T_c 's for the $4 \mu\text{m}$ photodoped wire width, we would expect the sharp onset at a width of $1.8 \mu\text{m}$ for the quasisaturated data to be shifted to a width $\sim 2.3 \mu\text{m}$ for the lower photodoping. From this result we conclude that the suppression of T_c is not related to the London penetration depth.

B. Inhomogeneous superconductors

It is well known that the intrinsic properties of the cuprates are sensitive to defects since they have a short coherence length¹⁶ and carrier densities near the metal-"insulator" transition.^{9,17} One type of defect which can degrade the intrinsic normal and superconducting properties in these samples is a grain boundary. During the growth of high- T_c films it has been shown that the films nucleate as grains with a screw location at the center of the grains.¹⁸ A grain boundary forms between adjacent grains.^{9,19} The grain sizes in these films were measured using an atomic force microscope (AFM) to be approximately 300 nm ; we would therefore expect, at most, 35 grain boundaries across the width of the sample.

As shown by high- T_c films grown on bicrystal grain boundary substrates, weak links are formed at grain boundaries. At these grain boundaries an insulating layer with a boundary resistivity of $10^{-9}\text{--}10^{-7} \Omega \text{ cm}^2$ is formed for optimally doped YBCO.^{9,17} Since the films studied in this work have been oxygen-depleted close to the metal-insulator transition, we expect that a greater degradation of the measured normal and superconducting macroscopic properties will occur at these grain boundaries than would be seen in optimally doped samples.

To explain the suppression of T_c for narrow photoinduced wires, we propose that the sample has superconducting grains connected by a random distribution of weak links. Since the weak links have different dimensions, they will have different critical currents as well. In this model the grains are superconducting at a temperature above the measured T_c . The measured T_c occurs at a lower temperature, at which point thermal fluctuations,²⁰ which fundamentally modify the V - I characteristics of the weak links, are no longer producing dissipation in the V - I measurements.

One motivation for ascribing the inhomogeneities to a distribution of weak links in these samples is the measurement of the critical current versus temperature. It was found that the critical current versus temperature for these samples had the form

$$I_c(T) \propto \left(1 - \frac{T}{T_c}\right)^m \quad (1 < m < 2), \quad (1)$$

where $m \approx 1$ for samples doped close to the metal-insulator transition, like sample B, and $m \approx 2$ for samples doped further from this transition, like sample A. This form for the temperature dependence of the critical current in Eq. (1) is a signature of weak links,^{19,21} where the exponent $m=2$ would be the expected value for a superconducting-normal-superconducting junction and $m=1$ would be the expected exponent for a superconducting-insulating-superconducting junction.²²

Gross *et al.*²³ have modeled the resistance versus temperature, near the superconducting transition temperature, for a single optimally-doped YBCO grain-boundary Josephson junction using an Ambegaokar-Halperin thermally activated phase slip theory.²⁰ In their analysis they used the Ambegaokar-Halperin theory with a temperature-dependent critical current to fit the resistance versus temperature data near the superconducting transition temperature. Using the same parameter in the critical current fit, they then modeled the nonlinear V - I curves at lower temperatures and found a strong correlation between the model and the experimental data.

Following the procedure of Gross *et al.*, the resistance versus temperature in the superconducting transition region has been modeled for sample A using the Ambegaokar-Halperin equations and $I_c = I_o(1 - T/T_c)^2$, where I_o was the only free parameter. The best fits to sample A after photodoping the entire sample with 2.75 W min/cm^2 are shown in the inset of Fig. 5. The imperfection of the fit is attributed to the distribution of weak links in the sample, which was not taken into consideration in the model.

Using a value of $I_o = 8 \mu\text{A}$ for the best fit, the shape of the V - I curves at lower temperatures can also be self-consistently modeled using the Ambegaokar-Halperin equation. For example, at $T = 12 \text{ K}$, we would expect from the fit in Fig. 5 that $I_c = 4.6 \mu\text{A}$ and $\gamma = \hbar I_c / ekT = 18$. Figure 5 shows a V - I trace taken at 12 K (denoted as squares). Theoretical v - x curves for $\gamma = 9, 13, 17, 19, 21$, and 25 are overlaid on the data in Fig. 5, using different axes. While this procedure predicted the correct curvature for the measured V - I curve, a comparison of the experimental current to the

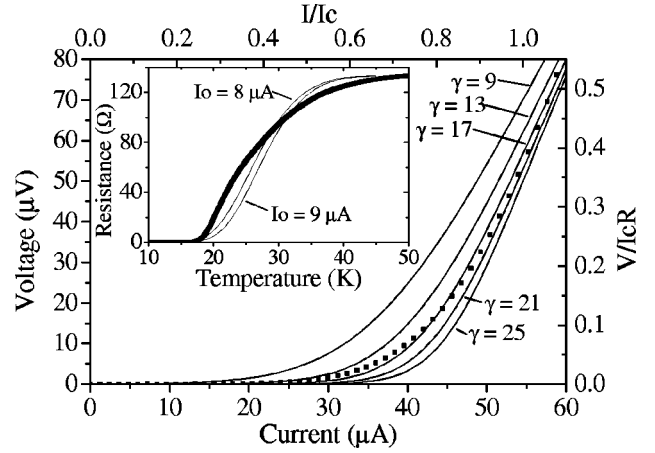


FIG. 5. Voltage versus current at $T = 12 \text{ K}$ for sample A. Lines are models of the data using an Ambegaokar-Halperin thermal activation theory for different values of $\gamma = \hbar I_c / ekT$. Inset of figure shows corresponding resistance versus temperature data with a critical current $I_c = I_o(1 - T/T_c)^2$ in the Ambegaokar-Halperin theory.

curvature of the model shows that the experimental current is approximately a factor of 10 larger than the theoretical value. At a temperature $T = 12 \text{ K}$ and a critical current of $50 \mu\text{A}$, a $\gamma = 200$ would have been expected. However, a $\gamma = 200$ would have a V - I curve closer to the zero temperature Josephson junction.

The discrepancy between the model and the measured critical current is because the measurement was not intrinsic to a single weak link as the analysis has assumed. Instead, a distribution of weak links is thought to cause the observed curvature. For example, if two Josephson junctions with the same critical current (I_c) are placed in a parallel circuit, then the total critical current of this double junction would be twice the critical current of a single junction. However, the voltage drop and curvature of the V - I curve would be the same as those of a single junction and a measurement of the critical current would predict a value for γ twice the value for a single junction. This type of behavior for the double Josephson junction follows our observed data. Ten Josephson junctions in parallel would be the requirement for sample A, in which the measured critical current was approximately a factor of 10 larger than the modeled critical current.

C. Classical percolation model

To further understand the wire-width-dependent suppression of T_c , we have developed a simple model based on classical percolation theory. A two-dimensional (2D) square bond lattice has been used in which the bonds connecting the sites have the same length and are randomly chosen to have a resistivity of either zero (superconducting) or one (dissipative). While this model clearly oversimplifies both the geometry of the grain structure and the behavior of the weak links, it captures some of the salient features of the data.

We begin by modeling the superconducting transition to extract a parameter that will be used in calculating the width of the percolative path. Based on percolation theory, the resistivity ρ of a random mixture of superconducting elements

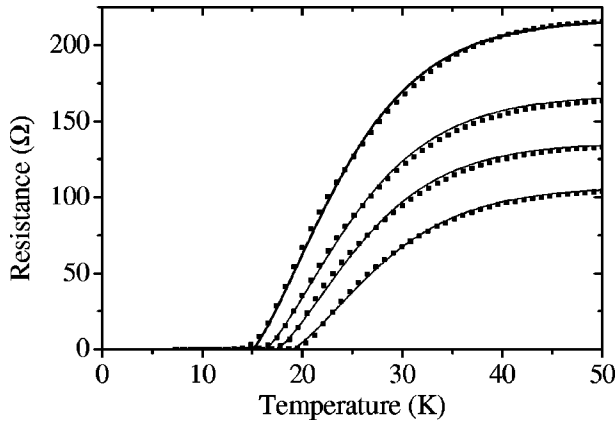


FIG. 6. Model of the superconducting transition for sample A at different integrated photon densities using a classical bond percolation model.

with fraction p can be written near the percolation threshold (p_c) as²⁴

$$\rho \propto (p_c - p)^s, \quad (2)$$

which goes to zero as $p \rightarrow p_c^+$. In two dimensions, the absolute value of the exponent s has been shown to be the same as for an insulating-conducting mixture when identical lattices are compared; that is, an exact duality exists between the insulating-normal conducting mixture and the superconducting-normal mixture.²⁵ For the 2D square bond lattice, the percolation threshold is $p_c=0.5$ and the critical exponent has been estimated to be 1.1–1.5.^{24,26,27}

In modeling the data it is assumed that the fraction of superconducting bonds (p) is increased by lowering the temperature. To model the resistance versus temperature curves in the superconducting transition region, the following model will be used for the fraction of superconducting bonds as a function of temperature:

$$p(T) = 0.5 + 0.5 \tanh\left(\frac{T_c - T}{\Delta T}\right). \quad (3)$$

Equation (3) was chosen because of its simple form and because in the limit of a perfect homogeneous sample such that $\Delta T \rightarrow 0$, $p=0$ for $T \geq T_c$ and $p=1$ for $T \leq T_c$, which would be the expected result.

Substituting Eq. (3) into Eq. (2) and using a critical exponent of 1.25, the parameter ΔT can be adjusted to fit the data. Figure 6 shows the result of modeling the resistance versus temperature in the transition region for sample A at different levels of photodoping the entire sample. For these fits, a $\Delta T=12.5$ –13 K was used and, as shown, fits the data in the superconducting transition region quite accurately.

While Eqs. (2) and (3) can model the superconducting transition for wide samples, these equations do not explain the suppression of T_c for narrow wires. To gain some qualitative insight into the dependence on T_c versus the wire width, a simulation of the percolative path through a bond lattice was studied.²⁸ In this simulation, each bond was assigned a random value for T_c taken from a distribution based on Eq. (3). For a lattice of dimensions large compared to the

critical percolation width, the T_c of the lattice is determined on average by T_c of the distribution. If instead the width of the lattice is decreased, the T_c is found to decrease.

To further quantify this model, we have assigned a probability that each bond is normal and have counted up the different permutations by which a superconducting path can be broken. For example, assume that the probability for any bond in the lattice being normal is $\epsilon(T)$ and assume the lattice has n columns and m rows (we imagine that the current flows from the first column to the n th column). The lowest order term to break a continuous (superconducting) path would have an entire column normal. Since there are m rows, the probability of one column being blocked is ϵ^m . This type of break could occur in any of the n columns, thus the total probability for a continuous path being broken is $n\epsilon^m$.

By summing the probabilities for all of the different permutations, a continuous path across the bond lattice can be broken, and by setting that sum equal to a total probability P , T_c as a function of wire width can be calculated. If $P > P_c = 1/2$ ($P < P_c = 1/2$), the lattice would probably be normal (superconducting). For the first three terms (in powers of ϵ), $T_{c,m}$ as a function of m can be calculated by solving for T in the following equation:

$$P_c = \frac{1}{2} = n\epsilon(T)^m + 2(n-1)(m-1)\epsilon(T)^{m+1} + 2(n-1)(m-2)\epsilon(T)^{m+2} + 2(n-2)(m-2)\epsilon(T)^{m+2}. \quad (4)$$

To be consistent with the fits to the superconducting transition, $\epsilon(T) = 1 - p(T) = 0.5 + 0.5 \tanh[(T - T_c)/\Delta T]$ has been used with the values T_c and ΔT obtained from those fits. The lines in Figs. 3 and 4 show this percolation model for samples A and B, respectively, where the number of rows (m), which represents the wire width, has been adjusted to approximately fit the data. The modeling suggests that the number of inhomogeneities across the width of the sample is approximately 10 which is in good agreement with the number of grains across the width of the sample observed by AFM and with the Ambegaokar-Halperin model.

As the data on the two samples presented in Sec. III demonstrate, there is a sample-dependent variation in the critical percolation width. On the other hand, the classical percolation model developed here is for a statistical average of samples. Another shortfall of the square lattice percolation model is that it is not meaningful for lattice widths of the order of the bond length. A more realistic model would include a distribution of the sizes of the grain.

V. CONCLUSION

We have observed a suppression of the superconducting transition temperature for narrow photodoped wires. We have attributed this suppression to an inhomogeneous distribution of weak links in the films. This hypothesis is supported by a classical bond percolation model, an Ambegaokar-Halperin model, and critical current data. The density of weak links observed in this work, 1 weak link/ μm , is in good agreement with the density of weak links as measured by optical polarization microscopy reported

elsewhere.²⁹ Other mechanisms for the suppression of T_c do not appear viable.

One shortfall of the Ambegaokar-Halperin model presented in this article is that the percolative path for the current and the critical percolation width, which is the relevant information for these results, was not calculated. Haslinger and Joynt have recently calculated the V - I curves for a binary distribution of Josephson junctions at zero temperature.³⁰ It would be interesting to perform a similar calculation for the percolative path of current at finite temperatures.

ACKNOWLEDGMENTS

We would like to thank S. Kivelson (UCLA) and P. Lee (MIT) for discussions. We are grateful to B. Maiorov and E. Osquiguil (Centro Atómico Bariloche and Instituto Balseiro Argentina) for oxygen-depleting initial samples in this work and for providing us with valuable advice on performing the oxygen anneal. R. Decca (IUPUI) was involved in the early part of this work.

*Electronic address: bpalmer@lps.umd.edu

¹V. J. Emery and S. A. Kivelson, *Nature (London)* **374**, 434 (1995).

²T. Timusk and B. Statt, *Rep. Prog. Phys.* **62**, 61 (1999).

³Y. Wang *et al.*, *Science* **299**, 86 (2003).

⁴V. I. Kudinov *et al.*, *Phys. Rev. B* **47**, 9017 (1993).

⁵A. Gilibert, A. Hoffmann, M. G. Medici, and I. K. Schuller, *J. Supercond.* **13**, 1 (2000).

⁶D. Lederman, J. Hasen, I. K. Schuller, E. Osquiguil, and Y. Bruynseraede, *Appl. Phys. Lett.* **64**, 652 (1994).

⁷D. Lederman *et al.*, *J. Supercond.* **7**, 127 (1994).

⁸R. S. Decca, H. D. Drew, E. Osquiguil, B. Maiorov, and J. Guimpel, *Phys. Rev. Lett.* **85**, 3708 (2000).

⁹J. Halbritter, *Phys. Rev. B* **48**, 9735 (1993).

¹⁰E. Osquiguil, M. Maenhoudt, B. Wuyts, and Y. Bruynseraede, *Appl. Phys. Lett.* **60**, 1627 (1992).

¹¹M. Tetenbaum, B. Tani, B. Czech, and M. Blander, *Physica C* **158**, 377 (1989).

¹²G. A. Valaskovic, M. Holton, and G. H. Morrison, *Appl. Opt.* **34**, 1215 (1995).

¹³We define T_c as the point in temperature where the resistance is zero within the resolution of the measurement (10 m Ω).

¹⁴Y. J. Uemura *et al.*, *Phys. Rev. Lett.* **62**, 2317 (1989).

¹⁵R. I. Miller *et al.*, *Physica B* **326**, 296 (2003).

¹⁶G. Deutscher and K. A. Müller, *Phys. Rev. Lett.* **59**, 1745 (1987).

¹⁷H. Hilgenkamp and J. Mannhart, *Rev. Mod. Phys.* **74**, 485 (2002).

¹⁸M. Hawley, I. D. Raistrick, G. Beery, and R. J. Houlton, *Science* **251**, 1587 (1991).

¹⁹D. K. Lathrop, B. H. Moeckly, S. E. Russek, and R. A. Buhrman, *Appl. Phys. Lett.* **58**, 1095 (1991).

²⁰V. Ambegaokar and B. Halperin, *Phys. Rev. Lett.* **22**, 1364 (1969).

²¹J. Halbritter, *Phys. Rev. B* **46**, 14861 (1992).

²²P. G. de Gennes, *Rev. Mod. Phys.* **36**, 225 (1964).

²³R. Gross, P. Chaudhari, D. Dimos, A. Gupta, and G. Koren, *Phys. Rev. Lett.* **64**, 228 (1990).

²⁴H. J. Herrmann, B. Derrida, and J. Vannimenus, *Phys. Rev. B* **30**, 4080 (1984).

²⁵J. P. Straley, *Phys. Rev. B* **15**, 5733 (1977).

²⁶J. M. Ziman, *Models of Disorder* (Cambridge University Press, Cambridge, 1979).

²⁷R. Zallen, *The Physics of Amorphous Solids* (Wiley, New York, 1983).

²⁸B. S. Palmer, Ph.D. thesis, University of Maryland, College Park, 2003.

²⁹P. M. Shaldrin *et al.*, *IEEE Trans. Appl. Supercond.* **11**, 3226 (2001).

³⁰R. Haslinger and R. Joynt, *Phys. Rev. B* **61**, 4206 (2000).